

# LPE GROWTH AND SCINTILLATION PROPERTIES OF $A_2SiO_5$ (A=Lu, Gd, Y):Ce SINGLE CRYSTALLINE FILMS

**Y. Zorenko, V. Gorbenko, V. Savchyn, T. Voznyak.**

Department of Electronics, Ivan Franko National University of Lviv, Lviv, Ukraine

**B. Grinyov, O. Sidletskiy, A. Fedorov, V. Baumer.**

Institute for Scintillation Materials, Academy of Sciences of Ukraine, 61001 Kharkiv, Ukraine

**M. Niki, J. A. Mares,** Institute of Physics AS CR, 162 53 Prague, Czech Republic



LNU, Lviv, Ukraine



Institute for scintillation  
materials NASU



Institute of Physics AS CzR  
Prague, Czech Republic



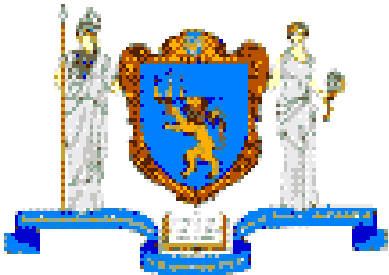
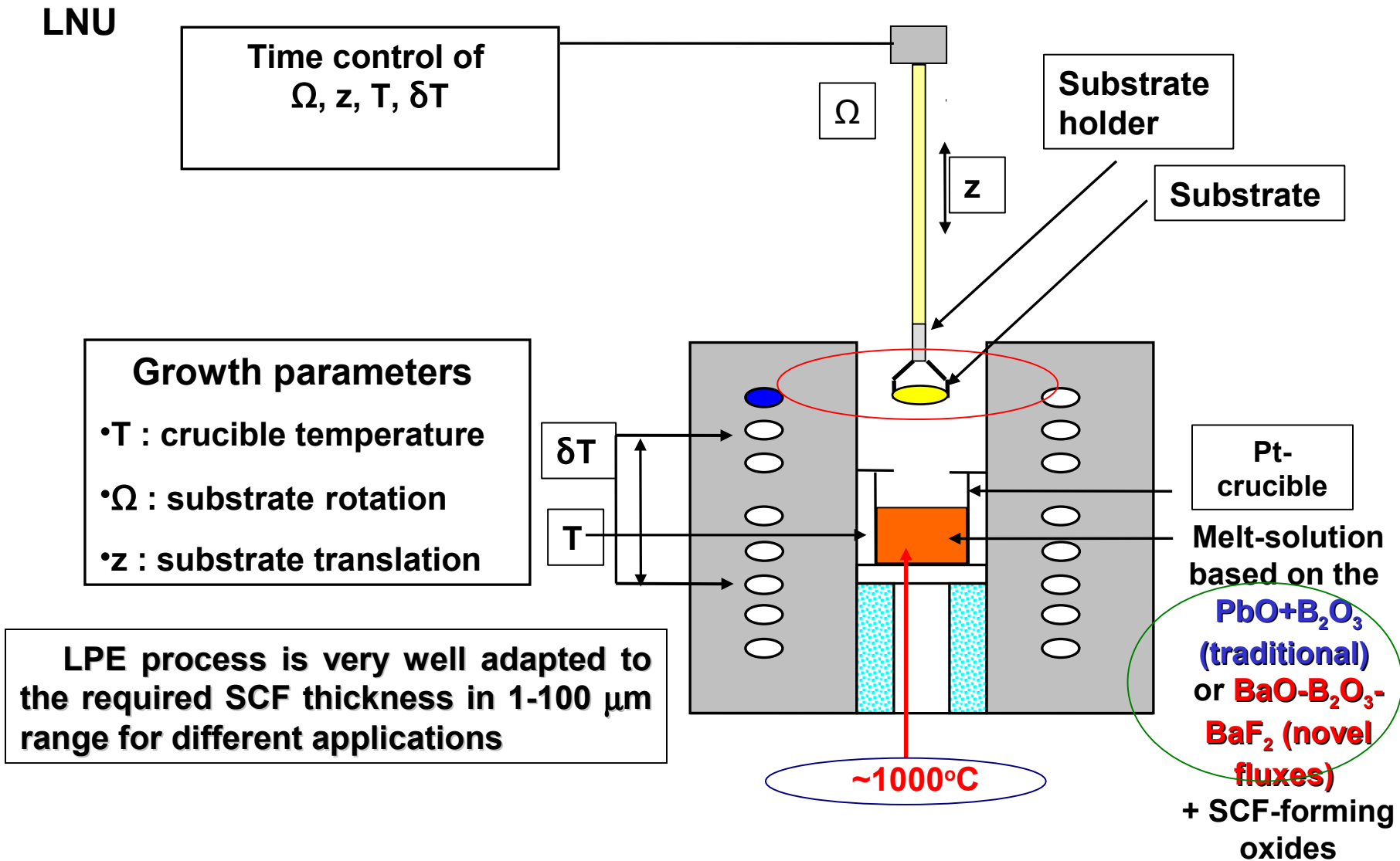
**ISMART 2010, 14-19.10.2010, Kharkiv, Ukraine**

# Outline

1. Introduction – shortly about the preparation of **single crystalline films (SCF)** by **Liquid Phase Epitaxy (LPE)** method and their application
2. Why we need the **blue or UV** emitting scintillators ?
3. Growth and luminescence properties of **undoped and Ce<sup>3+</sup> doped A<sub>2</sub>SiO<sub>5</sub> (A=Lu, Gd, Y) SCFs**
4. Luminescence of Pb<sup>2+</sup> ions in LSO SCF
5. Double doping and combined LSO based SCF scintillators
6. Conclusions

# 1. Growth of SCF scintillators by Liquid Phase Epitaxy (LPE) Method

Fig.1 Equipment for Liquid Phase Epitaxy (LPE) growth



LNU



LNU



## Application of phosphors based on the SCF of oxides

1. Thin-film scintillators for registration of  $\alpha$ - and  $\beta$ -particles
2. Combined scintillators for the registration of partial components of mixed ionizing fluxes
3. Screens for visualization of X-ray image with high spatial resolution
4. Cathodoluminescent (CL) screens of electron-beam tubes for raster scanning optical microscopes

# Recently developed visible-emitting SCF phosphors based on the Ce<sup>3+</sup>-doped YAG and LuAG garnets

YAG substrates with (111) or (100) orientation and diameter 1.5-65 mm

SCF thickness - 2-70  $\mu\text{m}$ ;

Temperature of growth 960-1050°C

Melt-solution based on **PbO-B<sub>2</sub>O<sub>3</sub>** flux

1. Best kinematic properties and solubility of oxides

2. **Pb<sup>2+</sup> ions in SCF are very effective quencher of the emission of rare-earth and other dopant in SCF !!!**

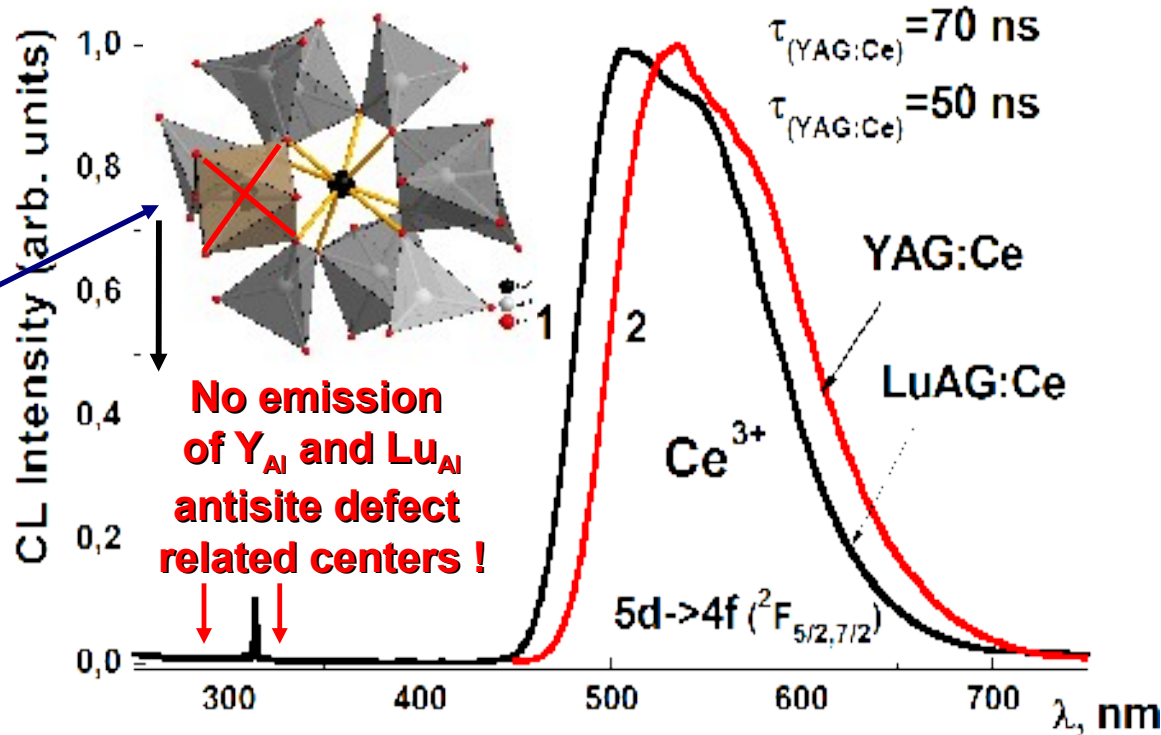


Fig.2. Cathodoluminescence (CL) spectra of YAG:Ce (1), LuAG:Ce (2) SCF, grown by LPE onto YAG substrates

Garnets	Relative LY, %	$\Delta E$ , %
<b>YAG:Ce film</b>	<b>100</b>	<b>11.5/8.5</b>
<b>YAG:Ce crystal</b>	<b>122</b>	<b>11</b>
LuAG:Ce film	118	9.5-10.5
LuAG:Ce crystal	122	12

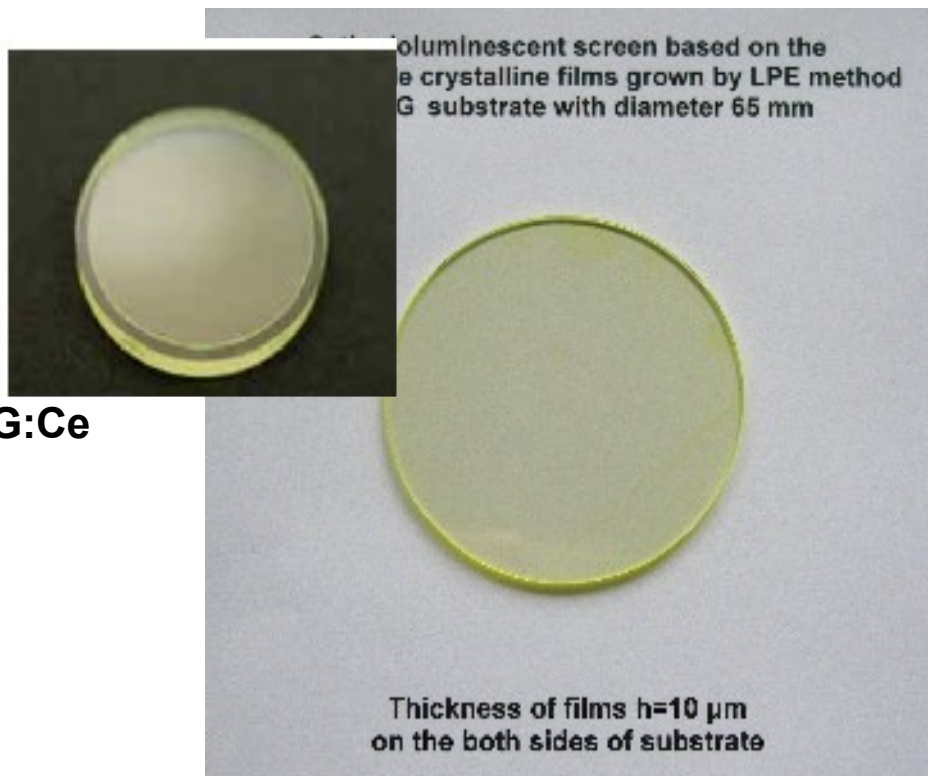
Table 1. LY and energy resolution of YAG:Ce and LuAG:Ce SCF in comparison with SC analogues under excitation by  $\alpha$ -particles of Pu<sup>239</sup> (5.15 MeV) source, measured using the detector based on the FEU 110 PMT ( $\lambda_{\text{max}}=450$  nm) in time gate of 0.5  $\mu\text{s}$ .



LOM,  
Lviv University

# Liquid Phase Epitaxy (LPE) technology

## Single crystalline film (SCF) scintillators and cathodoluminescent screens



LPE grown films LuAG:Ce and YAG:Ce  
SCF with different sizes

LuAG:Ce SCF ~ 25 μm

YAG substrate

Cleavage of LuAG:Ce/YAG  
epitaxial structure

# SCF screens for visualization of X-ray images

## Imaging with typical X-ray sources

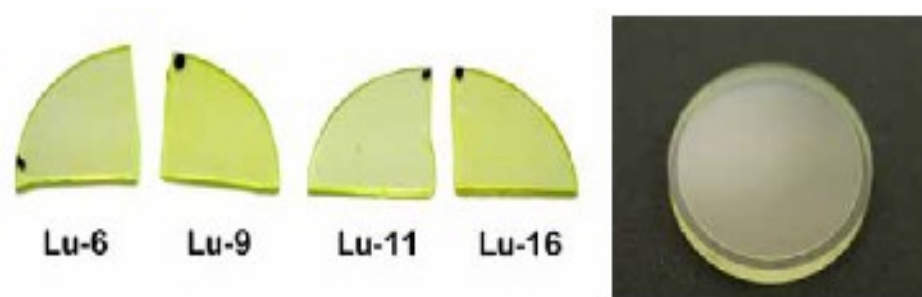


Fig. 19. Visual appearance of LuAG:Ce LPE-grown film samples Lu-6,9,11,16. On the right the bulk sample is displayed with the LuAG:Ce plate on the top surface.

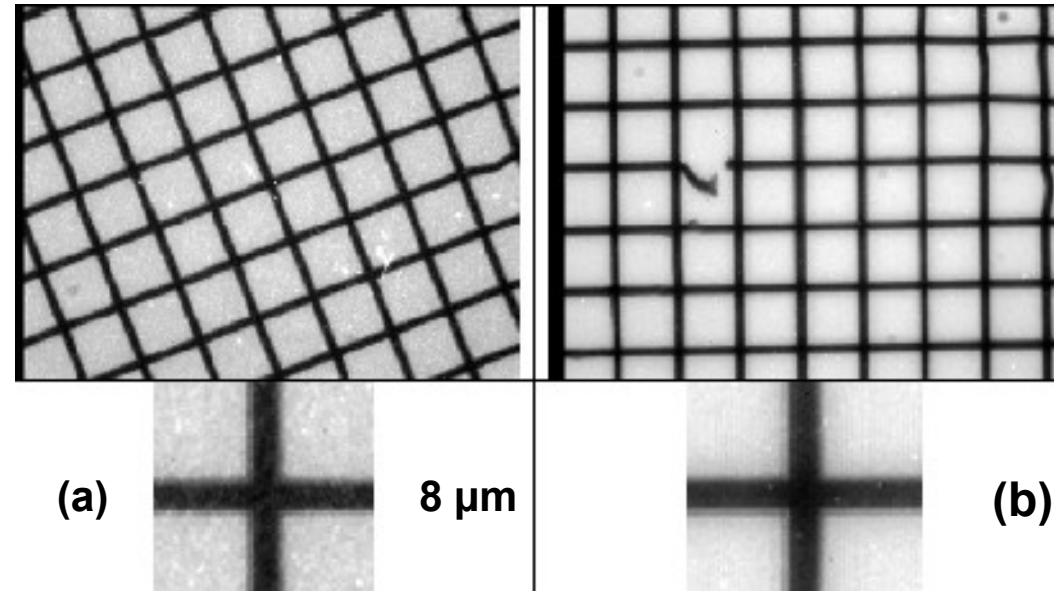


Fig.20. 2D X-ray imaging experiment is composed of microfocus X-ray source (on the left), sample holder and digital CCD camera with high 2D-resolution.

Fig.21. Image of Pt wire-net with thickness of  $\sim 8 \mu\text{m}$  obtained with help of **screens based on LuAG:Ce film (a) and crystal (b)** with thickness of  $\sim 20 \mu\text{m}$ . The images were obtained in Crytyr Ltd, Turnov, Czech Republic

**Film screen**

**Crystal screen**



# Microimaging at ESRF, Grenoble, France

## CCD Camera:

2kx2k; 12bit – 16 bit; fast (>5 fps...60 fps)

**OPTIC:** TOTAL MAGNIFICATION: x2.3 → x100;

pixel size ratio ~500

## SCINTILLATORS:

High X-ray absorption;

LY >15 Ph/KeV

Afterglow 4 decades@20 ms

Emission spectrum well overlapping with CCD camera sensitivity

High optical quality

Thickness from 1 μm up to 25 μm

## SPATIAL RESOLUTION:

up to 0.25-0.5 μm

## STATE OF THE ART

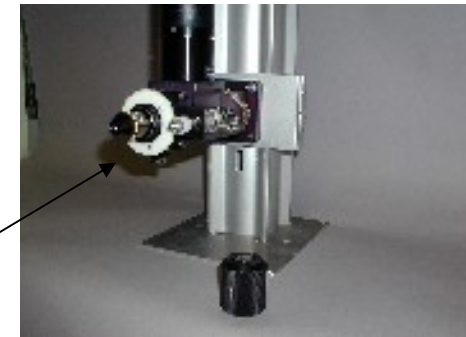
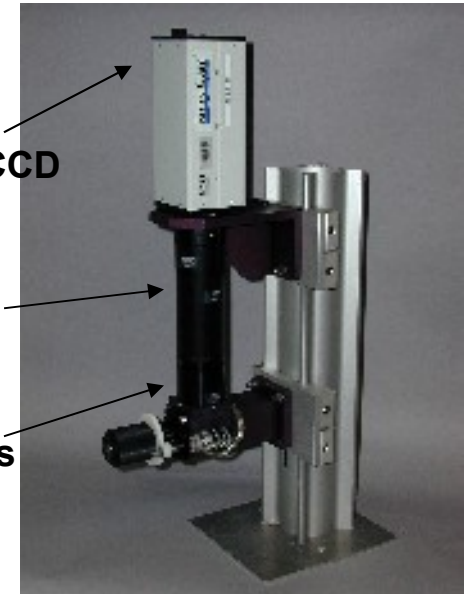
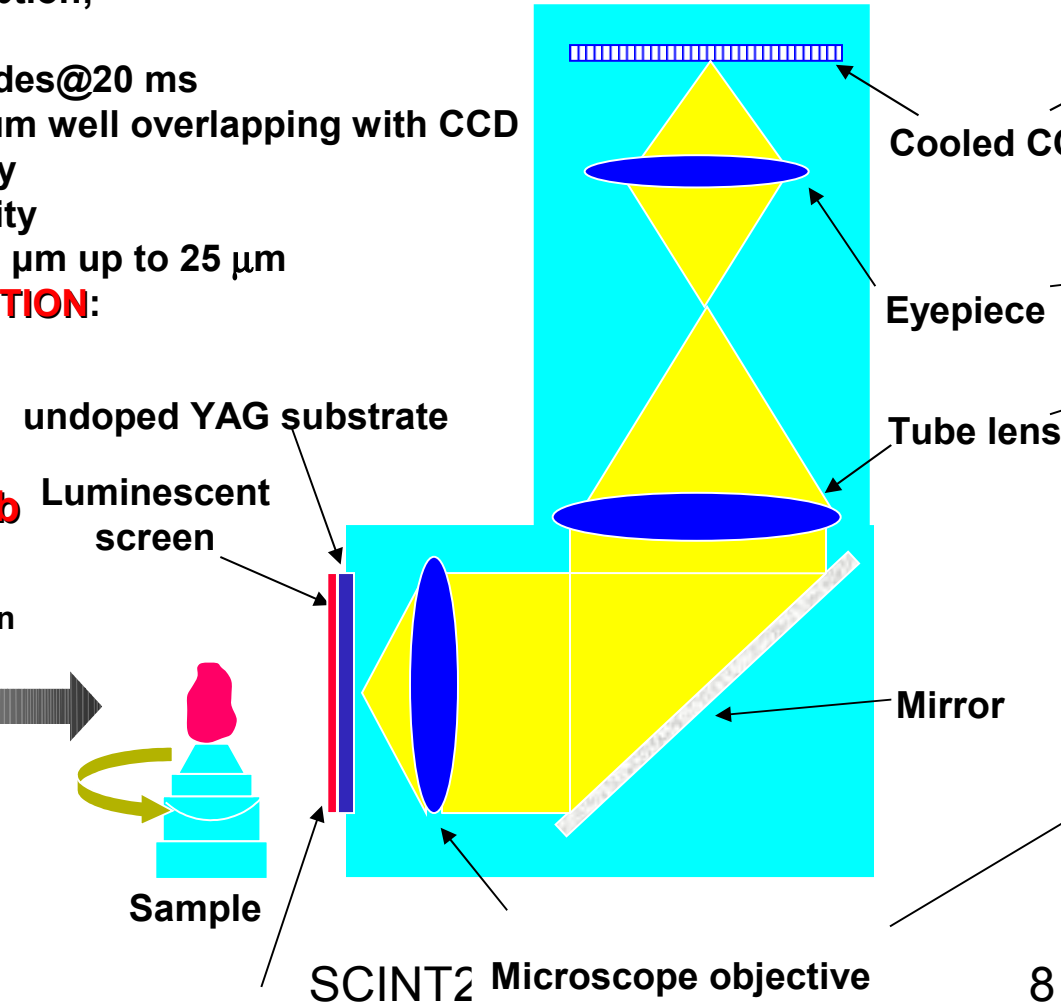
Fig.13. Scheme of X-Ray detector at ESRF

High X-ray absorption;  
LY >15 Ph/KeV  
Afterglow 4 decades@20 ms  
Emission spectrum well overlapping with CCD camera sensitivity  
High optical quality  
Thickness from 1 μm up to 25 μm

SPATIAL RESOLUTION:  
up to 0.25-0.5 μm

Firstly YAG:Ce,  
LuAG:Eu, GGG:Tb

X-rays or  
synchrotron radiation  
with E=5-10 eV



now LSO:Ce, LSO:Ce,Tb and LuAG:Sc, LuAG:Pr SCF

# Future development of SCF phosphors: Blue and UV emitting SCF phosphors

## Why do we need such phosphors?

1. The shift of emission spectra in the **blue or even UV** range can result in the increase of LY and energy resolution of **scintillators**.
2. Development of the raster optical microscope requires a **blue-UV cathode-luminescent light sources**, especially for the control of biological objects.
3. Using the **blue-UV-emitting** SCF can significantly improve the spatial resolution of **screens for visualization of X-Ray image** due to law for the spatial resolution limit for the optics  $R \sim 0.61\lambda/NA$ , where  $\lambda$  is the emission wavelength, NA is the numerical aperture of the optics.



In present work we considered the creation of new blue emitting SCF scintillators based on the **Ce<sup>3+</sup> doped LSO and LGSO ortosilicates**

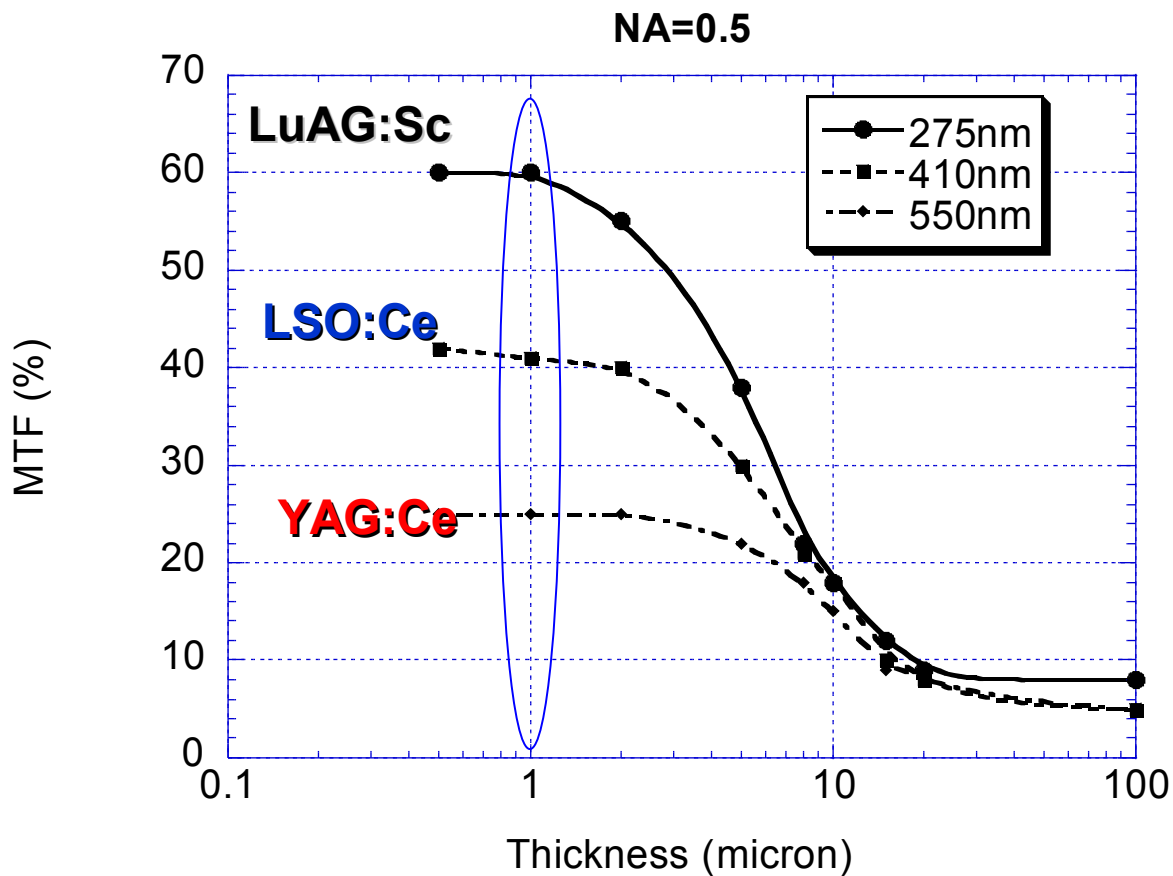


**Fig.1. Modulation Transfer Function (MTF's) for the imaging system with a numerical aperture of 0.5 and calculated at 1000 lp/mm.**

**The simulated curves were calculated for 275 nm, 410 nm and 550 nm emission lines of the different single crystalline film scintillators.**

For blue-UV emitting scintillators we need the materials with highest absorption ability of X-rays !!!

## X-rays absorption efficiency

$$\mu \sim \rho Z_{\text{eff}}^4$$

Crystal	$Z_{\text{eff}}$	$\rho$	$\rho Z_{\text{eff}}^{4*10^6}$
---------	------------------	--------	--------------------------------

<b>LSO</b>	<b>65.2</b>	<b>7.4</b>	<b>136</b>
------------	-------------	------------	------------

<b>LuAG</b>	<b>61</b>	<b>6.73</b>	<b>93</b>
-------------	-----------	-------------	-----------

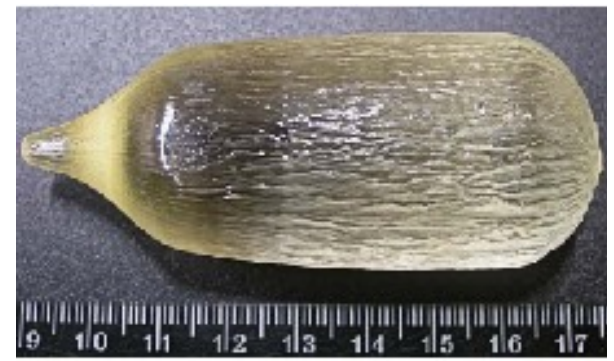
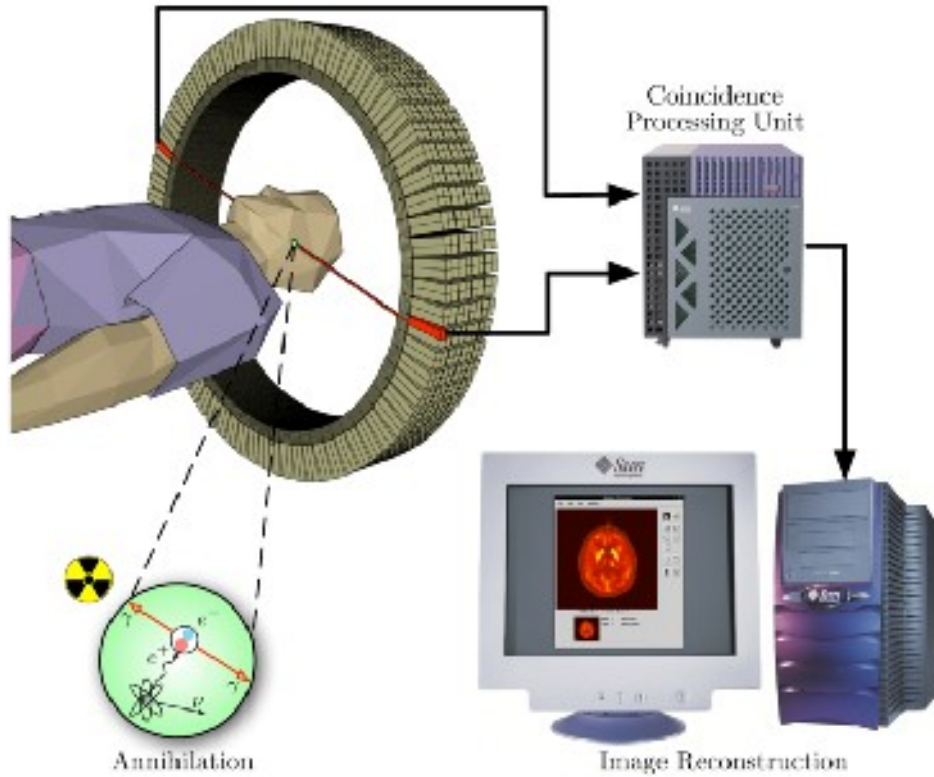
<b>LuAP</b>	<b>64.9</b>	<b>8.34</b>	<b>148</b>
-------------	-------------	-------------	------------

---

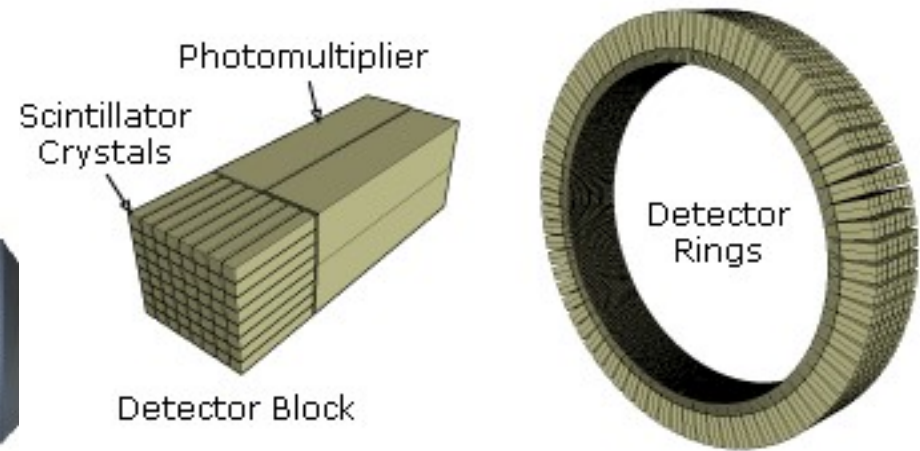
<b>YAP</b>	<b>34</b>	<b>5.5</b>	<b>7.35</b>
------------	-----------	------------	-------------

<b>YAG</b>	<b>32</b>	<b>4.55</b>	<b>5</b>
------------	-----------	-------------	----------

# Ce<sup>3+</sup> doped ortosilicates



(LuGd)<sub>2</sub>SiO<sub>5</sub>:Ce crystals



## Operation PET scanner

Recombination of positron + electron pair gives 2  $\gamma$ -rays of 512 keV under 180°.

The system detects pairs of gamma rays emitted indirectly by a positron-emitting radioisotope, which is introduced into the body. Images of metabolic activity (due to glucose with <sup>18</sup>F) in 3D are then reconstructed by computer analysis



LYSO:Ce crystals

**V<sub>o</sub>**

**(~ 95 %)**

**(~ 5 %)**

**(a few %)**

**Gd or Y doping caused the strong decreasing of the afterglow rate  
Gd doping make also the material of neutron-sensitive!**

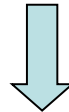
### **3. Growth and luminescence and scintillation properties of $\text{Ce}^{3+}$ doped $\text{A}_2\text{SO}_5$ (A=Lu, Gd, Y) SCF**

**We successfully crystallized by LPE**

- 1. LSO film onto LSO substrates**
- 2. LSO:Ce film onto LSO substrates**
- 3. YSO film onto YSO substrates**
- 4. YSO:Ce film onto YSO substrates**
  
- 5. LSO:Ce films onto YSO substrates**
- 6.  $(\text{Lu}_{1-x}\text{Gd}_x)\text{SO}:\text{Ce}$  film onto LSO substrates ( $x=0.2-0.7$ )**
- 7.  $(\text{Lu}_{0.2}\text{Gd}_{0.8})\text{SO}:\text{Ce},\text{Tb}$  film onto LSO substrates**

# LPE growth of LSO and LGSO based SCF

1. LSO and LSO:Ce SCF onto LSO substrates  
(homo-epitaxy, misfit film/substrate = 0)
2. YSO and YSO:Ce SCF onto YSO substrates  
(homo-epitaxy, misfit film/substrate = 0)
3.  $(\text{Lu}_{1-x}\text{Gd}_x)\text{SO}:\text{Ce}$  ( $x=0.2-0.7$ ) SCF onto LSO substrates  
(quasi homo-epitaxy, misfit film/substrate = - (0.55-1.36) %)
4. LSO and LSO:Ce SCF onto YSO substrates  
(quasi homo-epitaxy, misfit film/substrate = + 1.5 %)



Thus, we found

- that the LuSO and  $(\text{Lu}_{1-x}\text{Gd}_x)\text{SO}$  SCF can be grown onto significantly cheaper YSO substrates with same as LSO crystalline structure !
- the border condition for misfit film/substrate at crystallization of SCF of silicates is equal  $\pm 1.5 \%$ .
- This condition is very close to similar condition for SCF crystallization of perovskites and garnet compounds

## Segregation of RE ions in LSO SCF

From the content of several LSO:Ce, LGSO:Ce and LSO:Ce SCFs we estimated the segregation coefficient of  $\text{Ce}^{3+}$  and  $\text{Tb}^{3+}$  ions in these SCF been equal to  $\sim 0.0045$  and  $0.62$ , respectively.

The segregation coefficient of  $\text{Gd}^{3+}$  ions decrease from  $1.2$  up to  $0.48$  at the change relative Gd concentration x in MS from  $0.2$  to  $0.7$  per formula units  $(\text{Lu}_{1-x}\text{Gd}_x)_2\text{SiO}_5$ .

Such significant difference in the segregation coefficients of mentioned ions is due to respective difference in the ionic radii of  $\text{Ce}^{3+}$  ( $1.01 \text{ \AA}$ ),  $\text{Gd}^{3+}$  ( $0.94 \text{ \AA}$ ) and  $\text{Tb}^{3+}$  ( $0.92 \text{ \AA}$ ) in six-fold coordination in comparison with radius of  $\text{Lu}^{3+}$  ions in Lu2 ( $0.86 \text{ \AA}$ ) positions of LSO host.

### 3.1 Growth of LSO and LSO:Ce SCF onto LSO substrates (homo-epitaxy, misfit substrate / film = 0)

**Table 1 The growth condition of LSO and LSO:Ce SCF onto LSO substrates and LY of LSO:Ce SCFs in comparison with standard LSO:Ce and LYSO:Ce SC samples under excitation by  $\alpha$ -particles of  $\text{Am}^{241}$  (5.5 MeV) sources**

SCF samples content	Samples number	Ce content in MS/SCF, mole / at %	Lu/Ge ratio in MS	h, $\mu\text{m}$	fp, $\mu\text{m}/\text{min}$	Tg, °C	LY of RL, % $^{241}\text{Am}$ , 3 $\mu\text{s}$
Lu <sub>2</sub> SiO <sub>5</sub> (Pb)	a2	-	1:1	2.5	0.125	1015	27
	a3			5.5	0.046	1005	
	a4			6.0	0.033	997	
Lu <sub>2</sub> SiO <sub>5</sub> (Pb)	a5	-	1:1	7.2	0.06	1030	30
	a6			15	0.06	1015	
Lu <sub>2</sub> SiO <sub>5</sub> :Ce	b7	5	1:1	8.2	0.041	1005	62
	b8			6.7	0.035	1010	
Lu <sub>2</sub> SiO <sub>5</sub> :Ce	b9	10	1:1	5.9	0.02	1015	73
	b10			10	0.05	1005	
Lu <sub>2</sub> SiO <sub>5</sub> :Ce	b11	20	1:1	5.5	0.024	1015	110
	b12			5.4	0.03	1005	
Lu <sub>2</sub> SiO <sub>5</sub> :Ce	b13	14	2:3	21	0.12	1015	112
	b14			12.8	0.07	1025	
	b15			16	0.09	1020	
Lu <sub>2</sub> SiO <sub>5</sub> :Ce	b16	14	3:7	7.6	0.042	1030	142
Lu <sub>2</sub> SiO <sub>5</sub> :Ce SC (LuY) <sub>2</sub> SiO <sub>5</sub> :Ce	20-08 Cz-10	0.2 at.% Ce		0.6mm		2030	100 282

## Activator content and light yield (LY) of LSO:Ce SCF

LSO:Ce SCF grown from MS with 10 mole % CeO<sub>2</sub> concentration has the content of **Lu<sub>2</sub>SiO<sub>5</sub>:Ce (0.05 at. %)**, **Pb(0.02-0.033 at %)**.

Thus, the Pb/Ce ions ratio in these SCF is only **~1.5-2.5**. For comparison, the Ce/Pb ratio in the best YAG and LuAG:Ce SCF is **above 15-17** and at least on the one order higher than in LSO:Ce SCF !

**Therefore, the segregation coefficient of lead ions is one order higher at homo-epitaxial growth of LSO SCF onto LSO substrates than for the SCF of YAG and LuAG garnets grown onto YAG substrates**

### Local conclusions

- 1. LY of the best LSO:Ce SCFs samples is of 110-142 % of that for LSO:Ce counterpart under  $\alpha$ -particles excitation but is only ~ 40 % of that for best LYSO:Ce crystals due to the strong influence of lead contamination !!**
- 2. The reason for the large LY of LSO:Ce SCF with respect to the bulk crystal analogue even at such large Pb<sup>2+</sup> contamination is significantly lower concentration of oxygen vacancies in SCF scintillators due to lower temperature of their crystallization in oxygen-containing (air) atmosphere.**

# Comparison of CL spectra of LSO:Ce SCF and SC

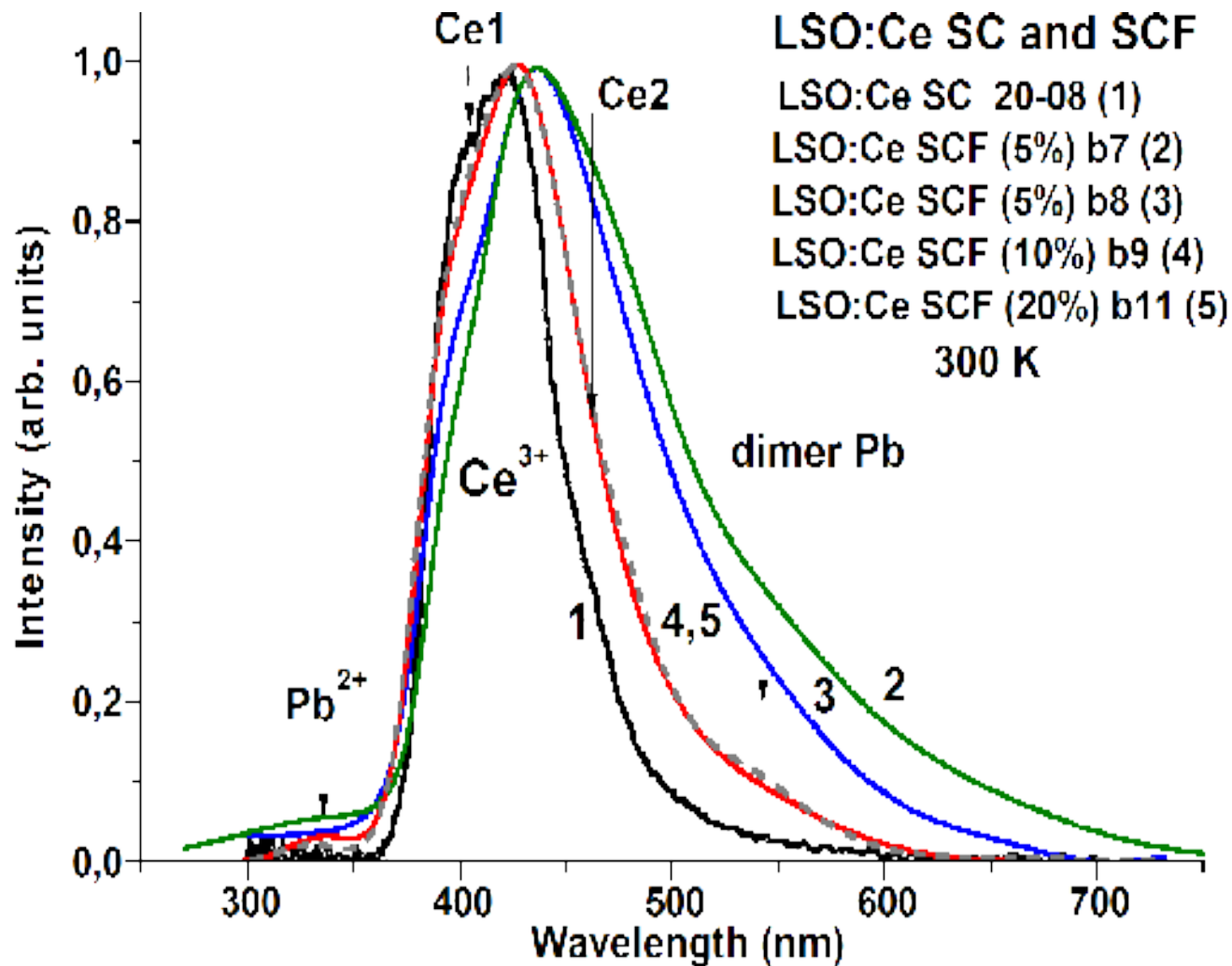


Fig.3. Normalized CL spectra of LSO:Ce SCF (2-5) grown at CeO<sub>2</sub> content in MS of 5 mole % (2, 3), 10 mole % (4) and 20 mole % (5) and different temperatures of growth (curve 2 and 3) in comparison with CL spectrum of LSO:Ce SC (1). T=300 K

**The CL spectra of LSO:Ce SCF is systematically red shifted with respect to the CL spectra of bulk single crystal counterpart !**

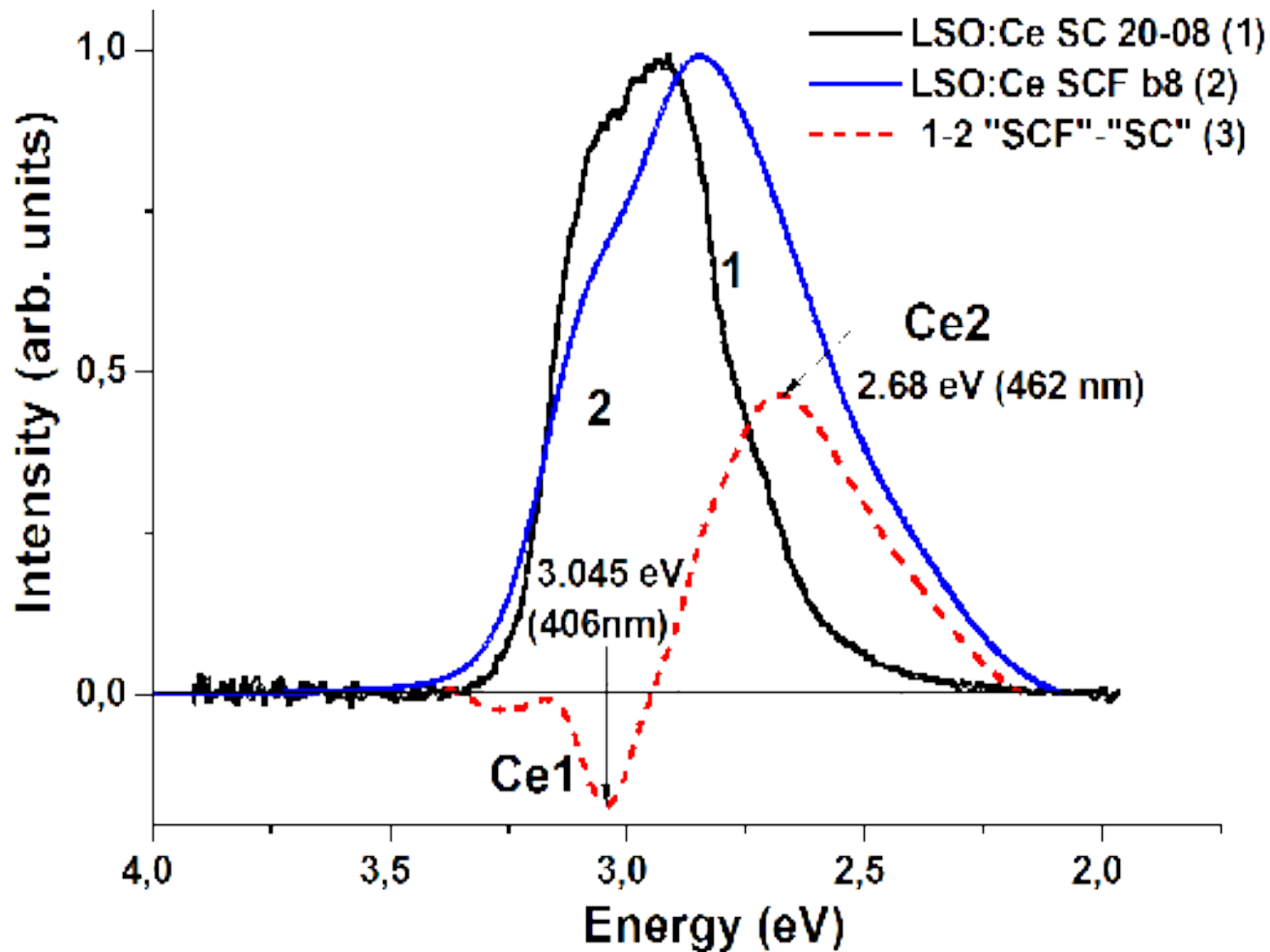
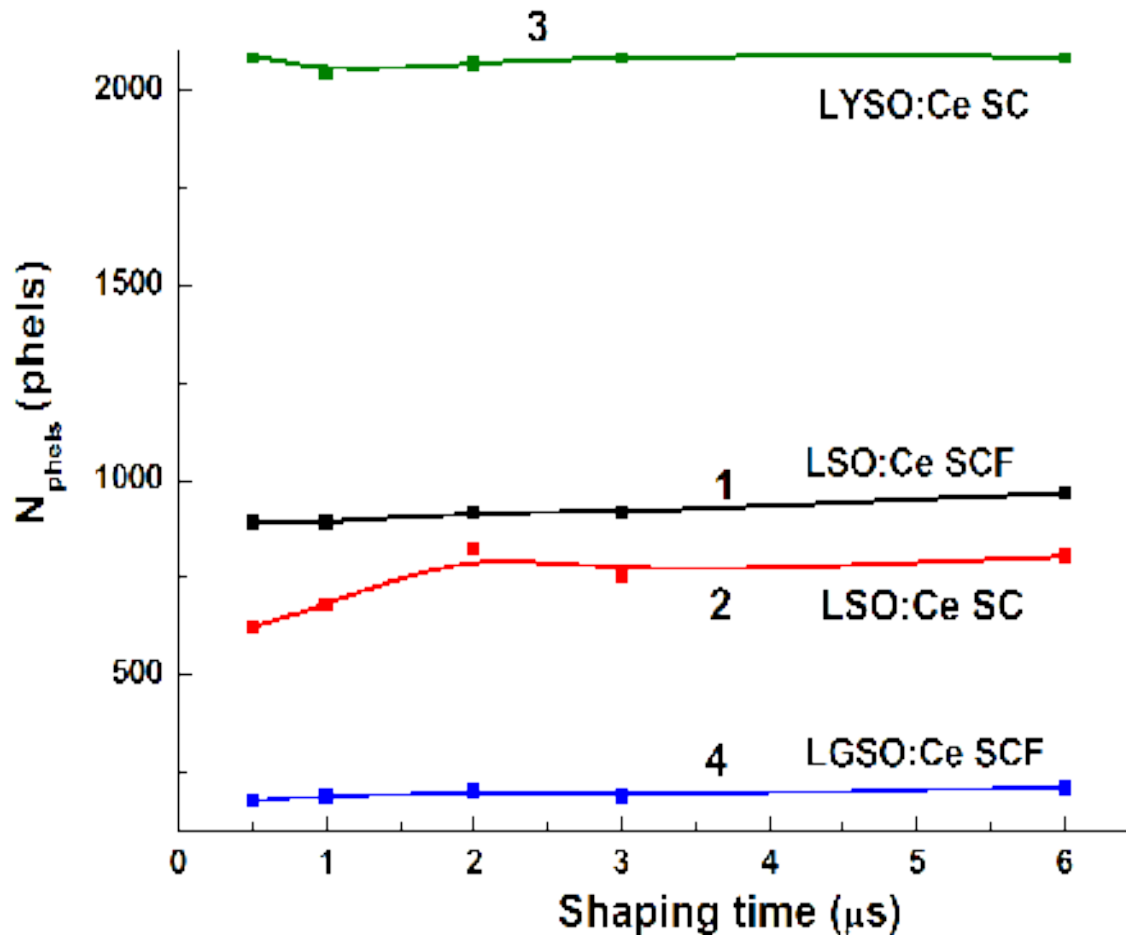


Fig.4. Module of difference (curve 3) between the normalized CL spectra of LSO:Ce (20 mole %) SCF (curve 1) and SC (curve 2).



Dependence of LY  $N_{\text{pheIs}}$  on shaping time of scintillation registration for LSO:Ce SCF(1) and LGSO:Ce SCF (4) in comparison with LSO:Ce 20-08 SC (2) and LYSO:Ce SC (3)

**Dependence of LY on shaping time for LSO:Ce SCF is very flat (curve 1) and close for respective dependence in high quality LYSO:Ce SC (curve 3) where the influence of the oxygen vacancies on scintillation processes is strongly diminished.**

### 3.2 Growth of LuGdSO:Ce and LuGdSO:Ce,Tb SCF onto LSO substrates (homo-epitaxy, misfit substrate / film # 0)

Table 2 **The growth condition and LY of LGSO:Ce SCF** in comparison with the LY of the standard LSO:Ce and LYSO:Ce SCs under excitation by  $\alpha$ -particles of  $\text{Am}^{241}$ (5.5 MeV) source

SCF samples content	Samples number	CeO <sub>2</sub> content in MS, mole %	h, $\mu\text{m}$	T <sub>g</sub> , °C	LY RL, % <sup>241</sup> Am, 3 $\mu\text{s}$
Lu <sub>0.3</sub> Gd <sub>0.7</sub> SiO <sub>5</sub> :Ce	c1	1.5	3.5	1003	50
	c3		2.8	987	
	c4		3.2	998	
Lu <sub>0.5</sub> Gd <sub>0.5</sub> SiO <sub>5</sub> :Ce	d4	15	5.3	1000	57
	d5		4.7	994	
Lu <sub>0.6</sub> Gd <sub>0.4</sub> SiO <sub>5</sub> :Ce	d6	15	2.5	997	67
	d8		5.4	998	
Lu <sub>0.8</sub> Gd <sub>0.2</sub> SiO <sub>5</sub> :Ce	d11	15	8.0	993	77
	d12		11.5	1003	
Lu <sub>0.8</sub> Gd <sub>0.2</sub> SiO <sub>5</sub> :Ce,Tb	e1	15 + 15 (Tb <sub>4</sub> O <sub>7</sub> )	12	1005	68
Lu <sub>2</sub> SiO <sub>5</sub> :Ce	b14	14	12.8	1025	112
Lu <sub>2</sub> SiO <sub>5</sub> :Ce SC	20-08	0.2 at.% Ce	0.6 mm	2030	100
(LuY) <sub>2</sub> SiO <sub>5</sub> :Ce	Cz-10				282

**LY of (Lu<sub>0.3</sub>Gd<sub>0.7</sub>)SO:Ce SCF decrease with increasing the Gd content up to 65 % with respect to undoped LSO:Ce SCF**

## CL spectra of LGSO:Ce SCF

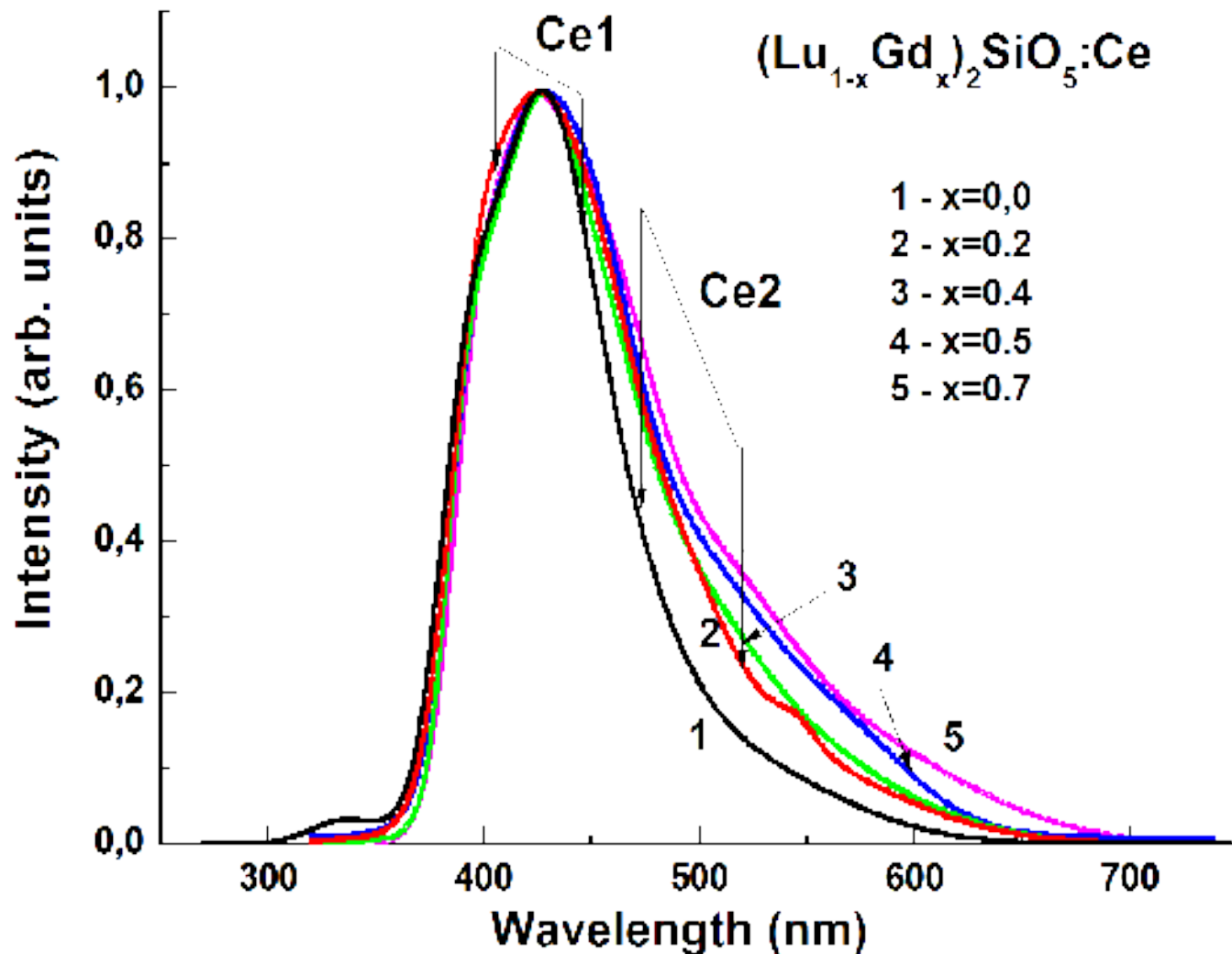


Fig.2 Normalized CL spectra of  $\text{Lu}_2\text{SiO}_5:\text{Ce}$  SCF (1) and  $(\text{Lu}_{1-x}\text{Gd}_x)_2\text{SiO}_5:\text{Ce}$  SCF (2-5) grown at different Gd content  $x=0.3$  (2), 0.5 (3), 0.6 (4) and 0.8 (5)

**The CL spectra of  $(\text{Lu}_{0.3}\text{Gd}_{0.7})\text{SO}:\text{Ce}$  SCF is systematically red shifted with increasing the Gd content up with respect to the  $\text{LSO}:\text{Ce}$  SCF due to redistribution of  $\text{Ce}^{3+}$  ions over Ce1 and Ce2 positions of  $(\text{Lu-Gd})\text{SO}$  host**

## Comparison of CL spectra of LuGdSO:Ce and LSO;Ce SCF

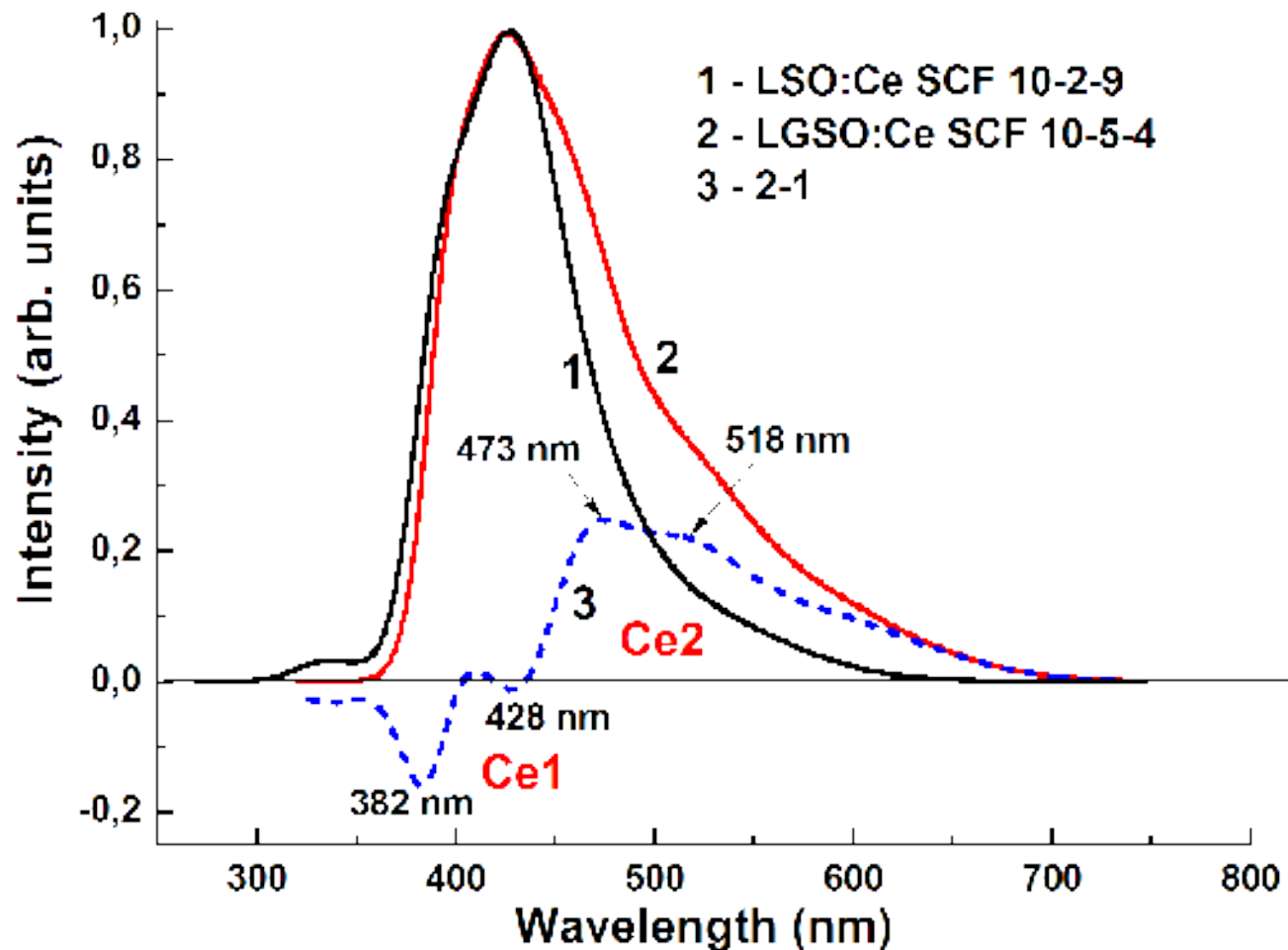


Fig.9 Normalized CL spectra of  $\text{Lu}_2\text{SiO}_5\text{:Ce}$  (1) and  $(\text{Lu}_{0.5}\text{Gd}_{0.5})_2\text{SiO}_5\text{:Ce}$  SCFs at 300 K and their difference (3). The extremes in the difference curve indicate the positions of Ce1 and Ce2 bands in LSO:Ce host

## **4. Luminescence of Pb<sup>2+</sup> ions in LSO SCF**

In nominally undoped LSO:Ce SCF grown from PbO-based flux we found the luminescence of Pb<sup>2+</sup> ions related to <sup>3</sup>P<sub>1</sub>-<sup>1</sup>S<sub>0</sub> radiative transitions both in Lu1 and Lu2 positions of LSO host

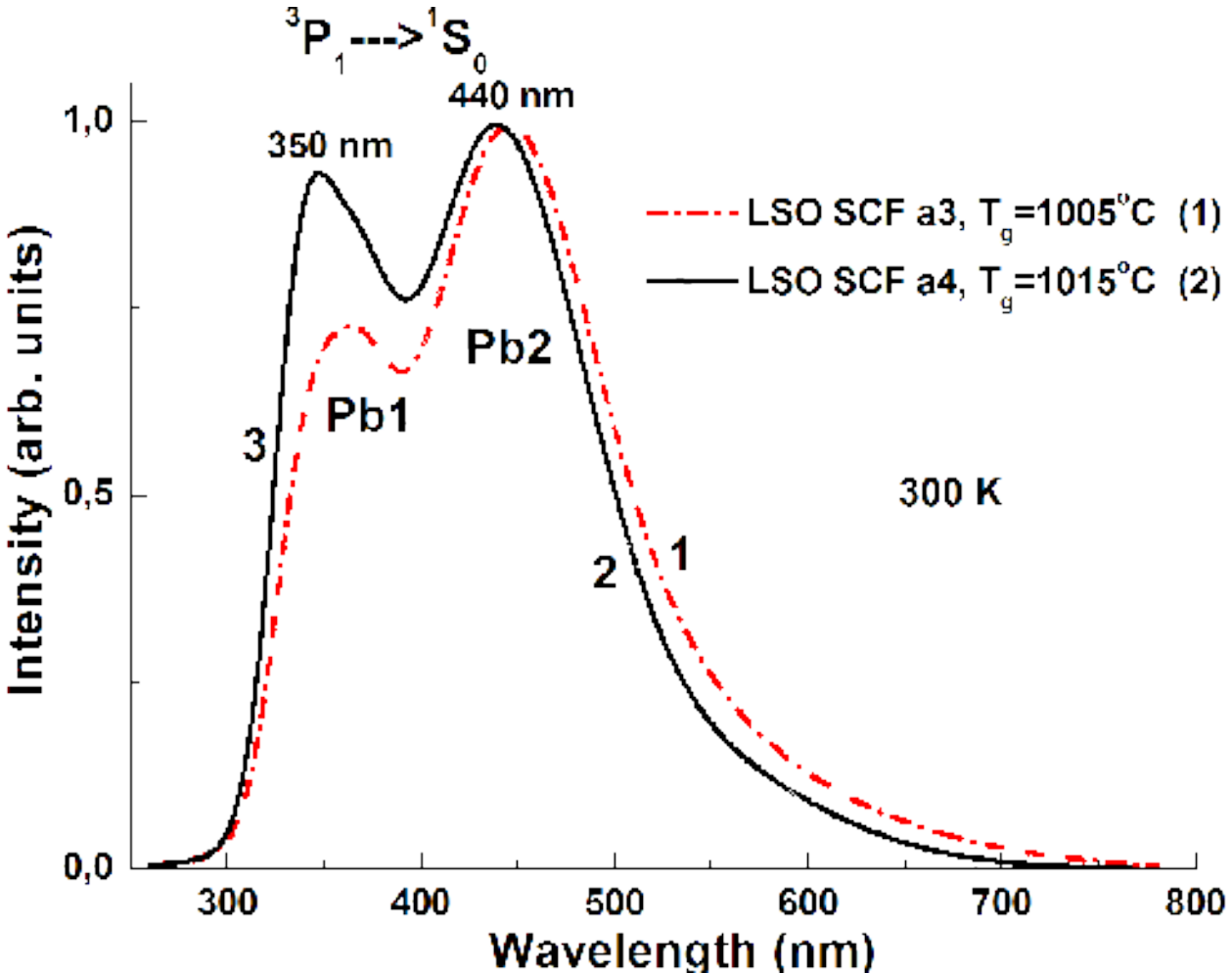
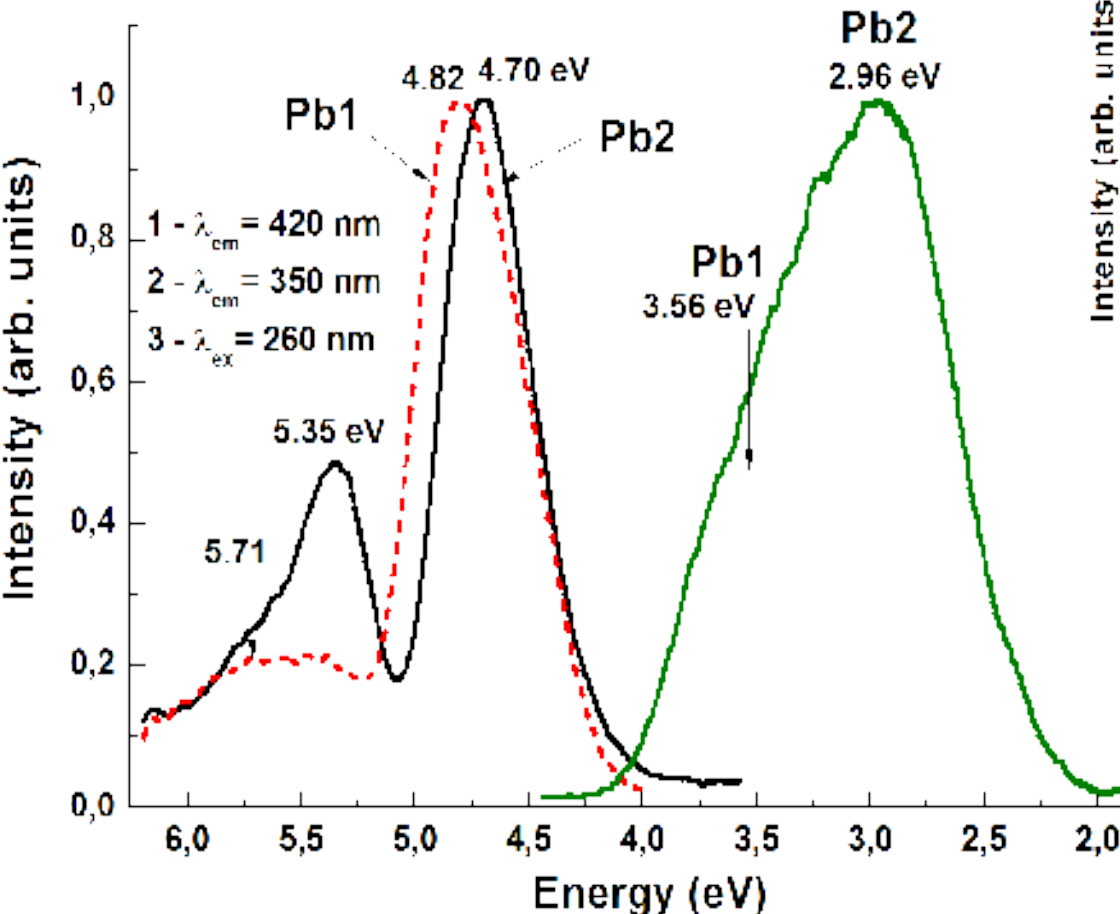


Fig.2 Normalized (on the maximum intensity of the main peak) CL spectra of nominally undoped LSO SCF a1, a2, a3 (curves 1-3, respectively) grown at different temperatures (see Table).

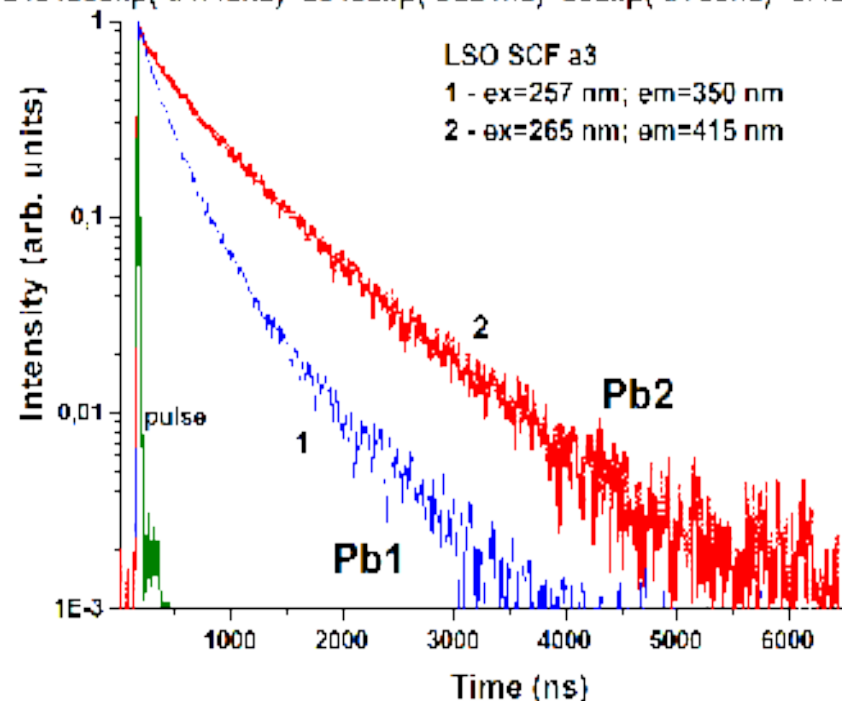
# Luminescence of Pb1 and Pb2 centers in LSO:Ce SCF



Excitation (1, 2) and PL (3) spectra of Pb<sup>2+</sup> luminescence in LSO SCF at registration of the emission at 340 nm (1) and 430 nm (2) and excitation at 260 nm (3)

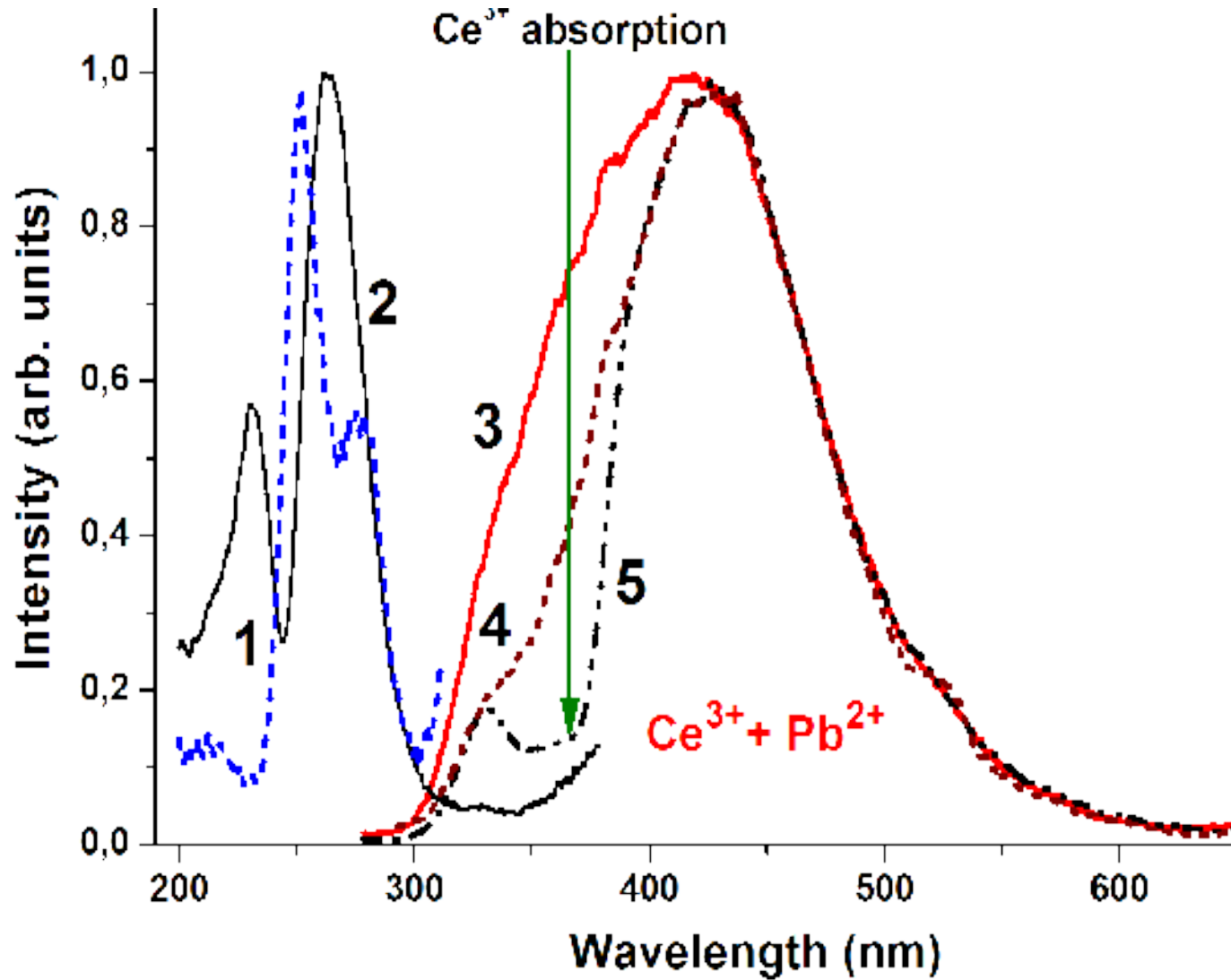
$$1 - I = 1709 \exp(-t/1.1 \text{ ns}) + 753 \exp(-t/444 \text{ ns}) + 314 \exp(-t/1077 \text{ ns}) + 0.58$$

$$2 - I = 245430 \exp(-t/1.45 \text{ ns}) + 2045 \exp(-t/221 \text{ ns}) + 83 \exp(-t/760 \text{ ns}) + 0.48$$



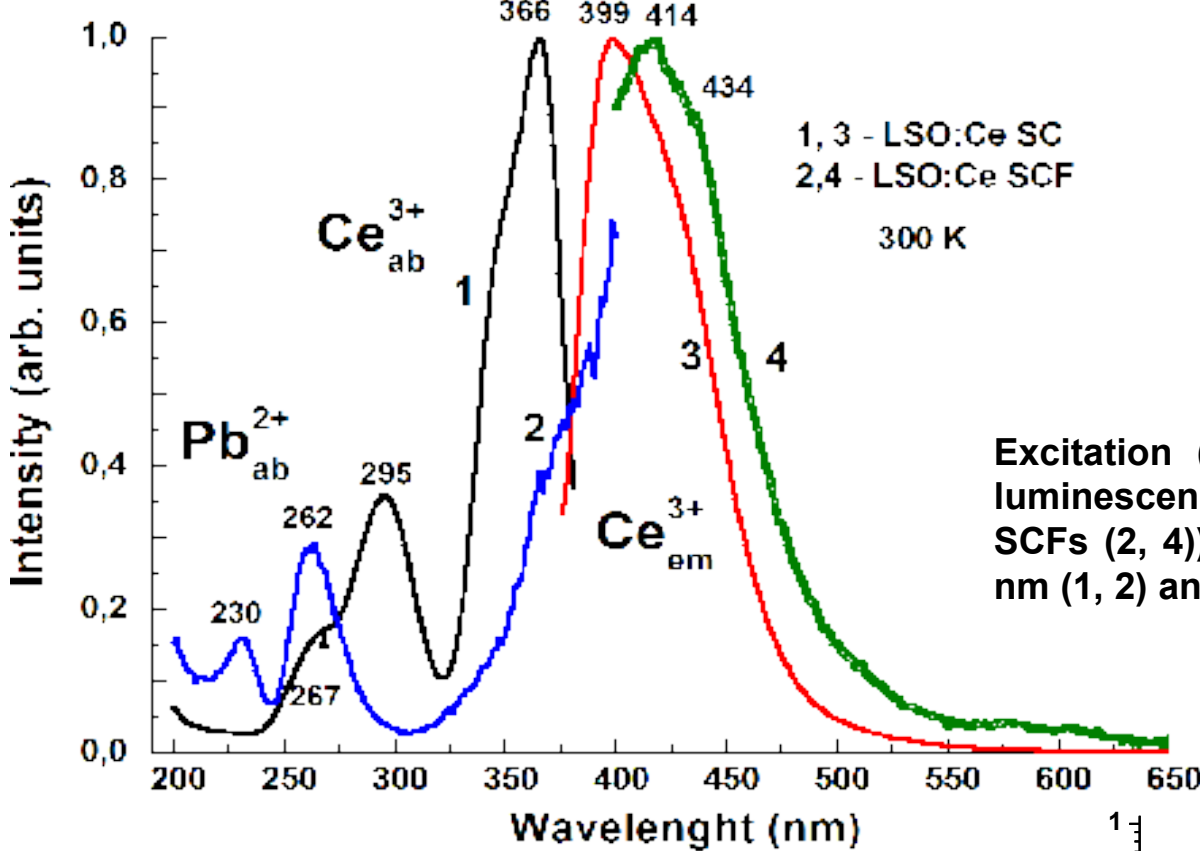
Decay kinetic of luminescence of Pb1 and Pb2 centers under excitation in corresponding A-bands of these centers at 265 nm (1) and 257 nm (2) and registration of emission at 415 nm (1) and 350 nm (2). The parameters of the three component fits of decay curves  $I(t) = \sum A_i \exp(-t/\tau_i) + \text{background}$  ( $i=1, 2$ ) is shown.

# $\text{Pb}^{2+} \rightarrow \text{Ce}^{3+}$ energy transfer in LSO:Ce SCF



Excitation (1, 2) and emission (3) spectra of  $\text{Pb}^{2+}$  luminescence in LSO SCF (1-3) and LSO:Ce (4, 5) SCF at registration of the emission at 330 nm (1) and 430 nm (2) and excitation at 260 nm (3-5)

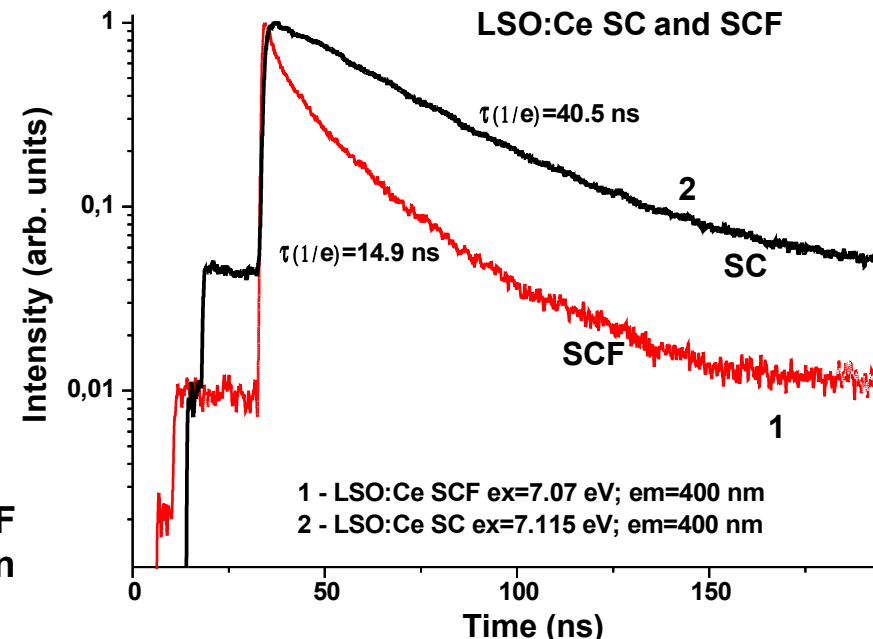
## Comparison of the excitation spectra and decay kinetic of LSO:Ce SC and SCF



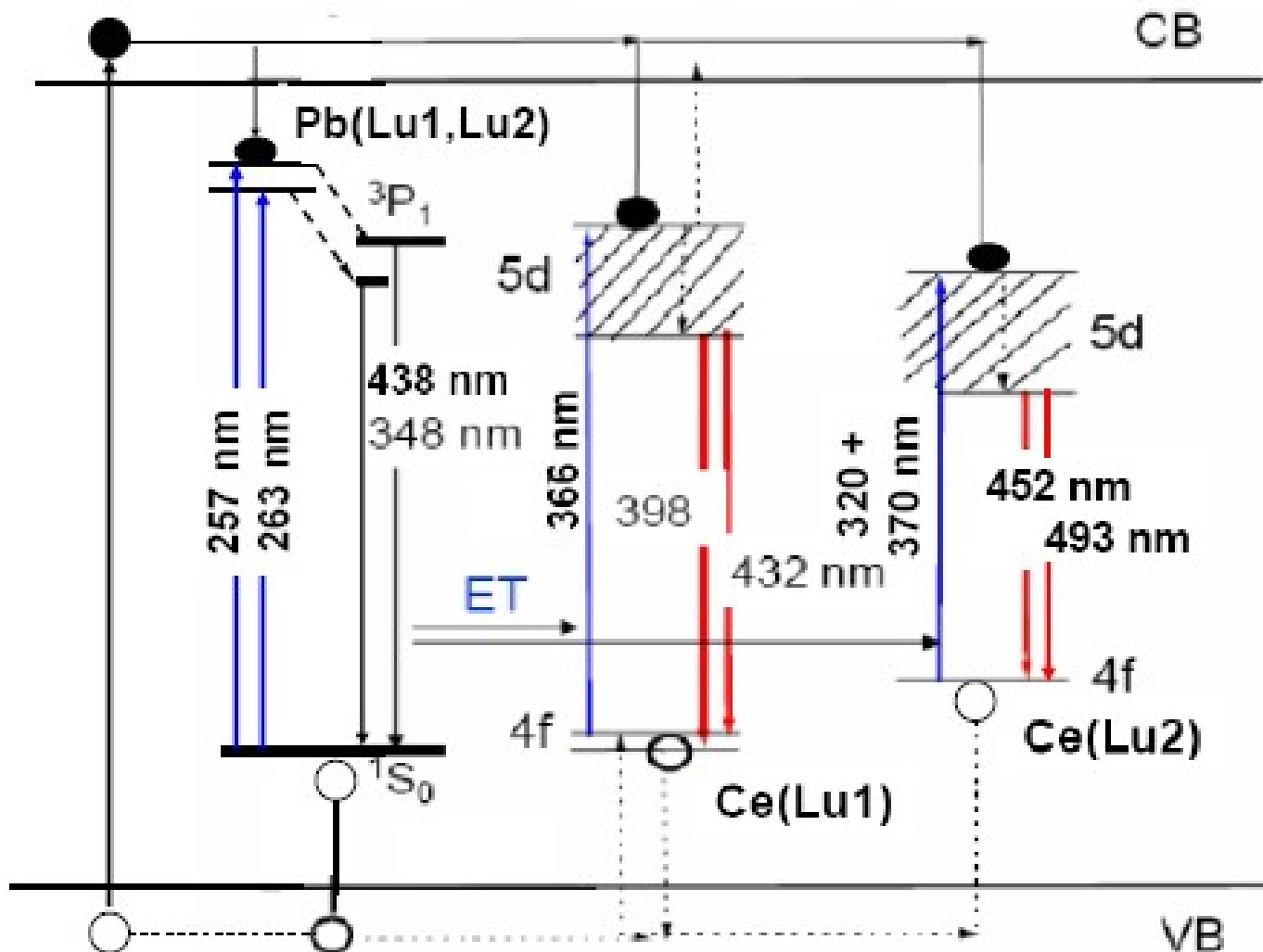
Excitation (1, 2) and PL (3, 4) spectra of  $\text{Ce}^{3+}$  luminescence in LSO:Ce SC (1, 3) and LSO:Ce SCFs (2, 4) at registration of the emission at 415 nm (1, 2) and excitation at 360 nm (3, 4)

**Complicated Pb-Ce-Pb energy transfer present in the LSO:Ce SCF !**

Decay kinetic of  $\text{Ce}^{3+}$  luminescence in LSO:Ce SCF (1) and LSO:Ce (2) SC under excitation in the exciton range at 7.07-7.15 eV (1, 2)

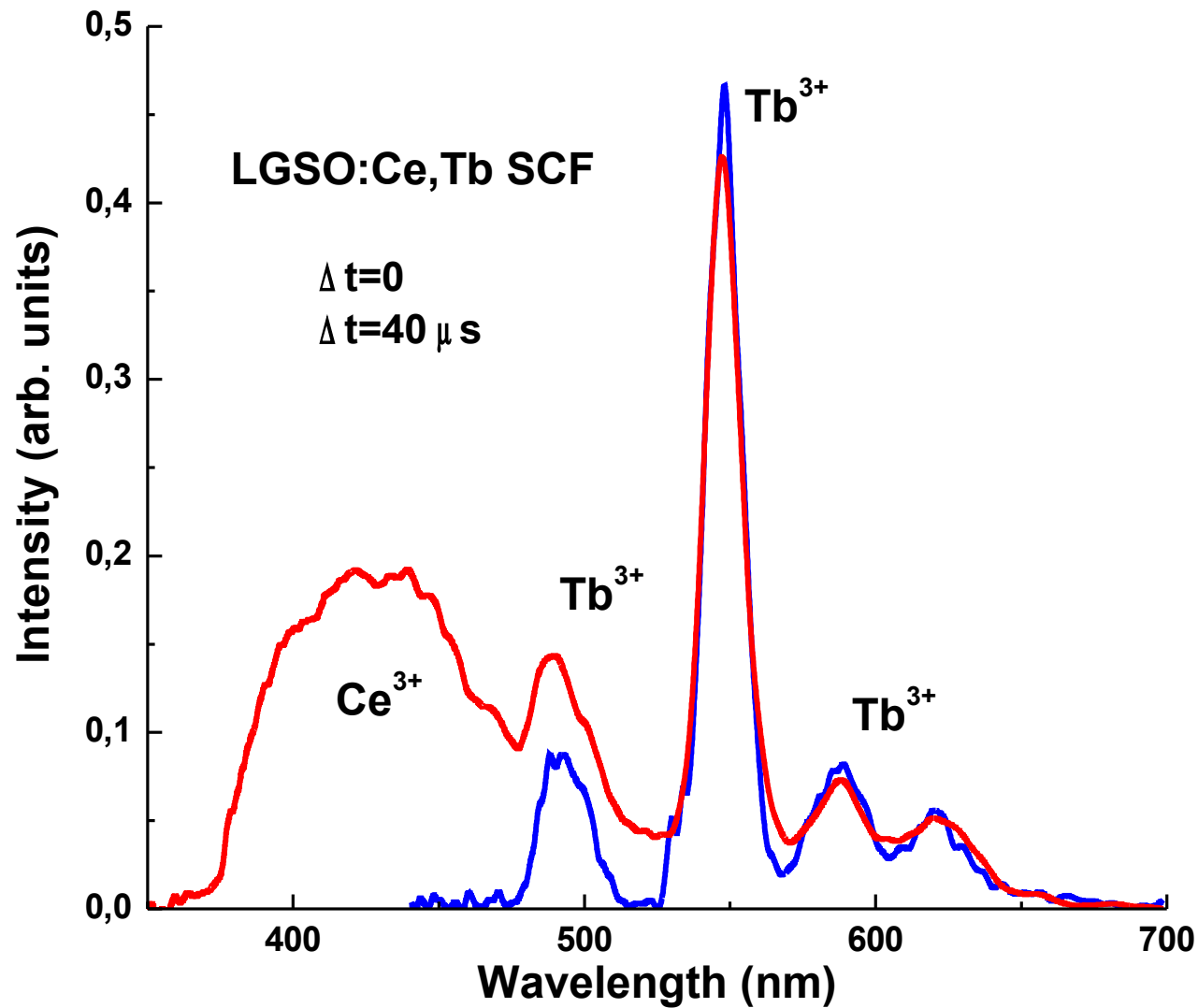


## Scheme of energy transfer processes in LSO:Ce SCFscintillators



**Scheme of optical transitions of Pb(Lu1) and Pb(Lu2) centers as well as Ce(Lu1) and Ce(Lu2) centers in LSO:Ce SCF at 300 K under the high-energy excitation and Pb-Ce energy transfer processes**

## 5. Double doping and combined LSO SCF scintillators

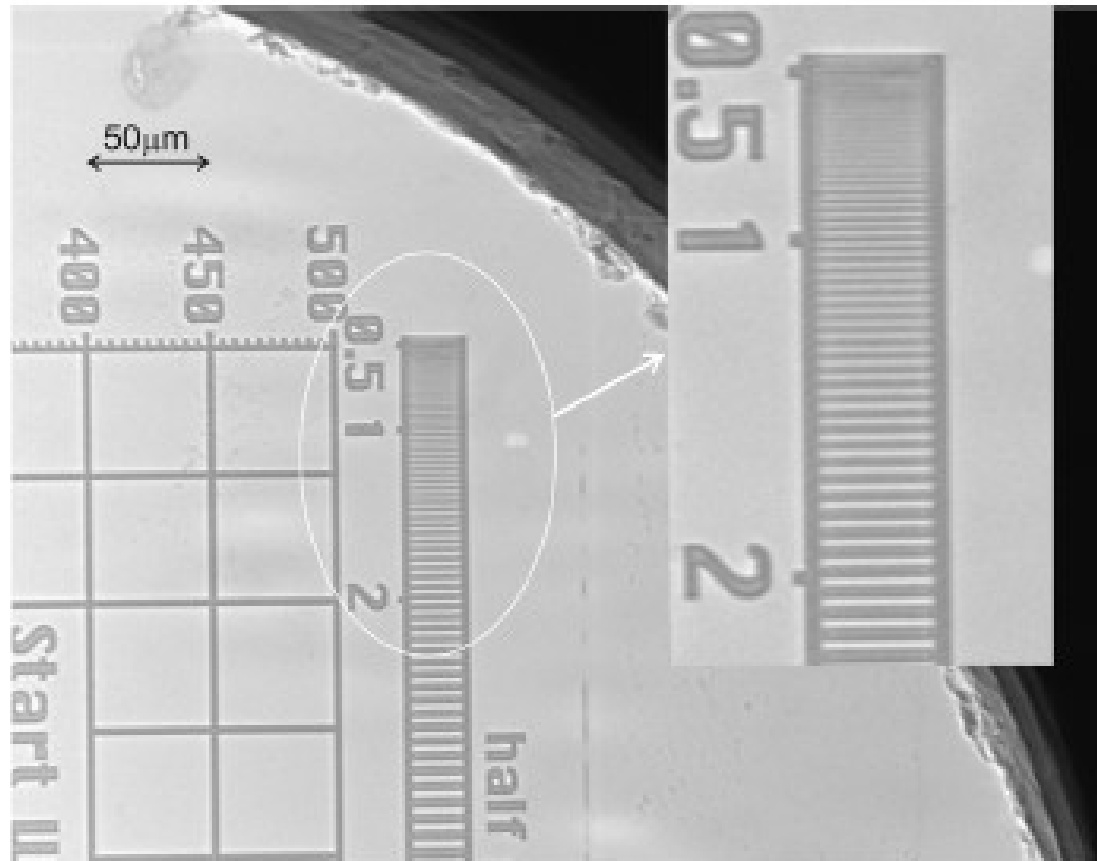


CL spectra of LuGdSO:Ce,Tb SCF at  $\Delta t=0$  and delay signal after  $40 \mu s$

# Visualization of X-Ray images with blue-UV-emitting SCF scintillators



## Imaging in visible-blue light



$R \sim 0.8 \mu\text{m}$

Images of resolution target obtained using the visible emission of LSO:Ce,Tb SCF scintillators [T. Martin, IEEE TNS 56 (2009) 1412-1418].

**P-A. Douissard, et al.**

**J. Syn. Rad., 17 (2010) 571**

**Volume image of the tarsus of a [honey bee](#) (*apis mellifera*), acquired by synchrotron microtomography. As an insect the honey bee has an external skeleton and the muscles are inside of the skeleton. Using the synchrotron radiation it is possible to perform the anatomical studies without sectioning in order to save the native structure. The inset shows parts of an X-ray test pattern in order to demonstrate the spatial resolution reached.**

# Conclusions



1. The single crystalline films (SCF) of undoped and  $\text{Ce}^{3+}$ -doped  $\text{Lu}_2\text{SiO}_5$  (LSO) and  $(\text{Lu}_x\text{Gd}_{1-x})_2\text{SiO}_5$  (LGSO) orthosilicates with a thickness of 2.5-21  $\mu\text{m}$  were crystallized by the LPE method from melt-solution based on  $\text{PbO-B}_2\text{O}_3$  flux onto undoped LSO and YSO substrates. These film are emitt in the blue range and can be used as scintillating screens for 2D X-ray microimaging.

2. *In case LGSO:Ce and LuSO:Ce film growth onto LSO and YSO substrates, respectively, we do not use any additional doping for reducing the misfit between the film and substrate lattices been equal of  $\pm 1.5\%$ .*

3. The luminescent properties of LSO:Ce and LGSO:Ce films grown from melt-solution with Ce content of  $\sim 0.05$  at. % were compared with properties of LSO:Ce (0.2 at. %) bulk crystal. *We found that the luminescence spectrum of LSO:Ce films caused by the  $5d^1-4f$  radiative transition of  $\text{Ce}^{3+}$  ions, is red-shifted in comparison with LSO:Ce crystals.* This a shift can be caused by different relative occupancy of Lu1 and Lu2 sites of LSO host by  $\text{Ce}^{3+}$  ions in the case of film and crystal due to very different temperatures for growth of crystal ( $2100^\circ\text{C}$ ) and film ( $\sim 1000^\circ\text{C}$ ).

4. *The light yield (LY) of LSO:Ce film overcome the LY of LSO:Ce bulk crystal by 10-40 % under excitation by  $\alpha$ -particles of  $\text{Am}^{241}$  sources (5.5 MeV) most probably due to very low concentration of oxygen vacancies in these films.*

# Conclusions



LNU



4. The luminescence spectrum of  $(\text{Lu}_{1-x}\text{Gd}_x)_2\text{SiO}_5:\text{Ce}$  films *is systematically red-shifted* with respect to spectrum of LSO:Ce films with increasing the Gd content in range of  $x=0-0.7$ . Such a red shift of the emission spectra of LGSO:Ce films is accompanied with the decreasing of their LY up to 65 % for  $(\text{Lu}_{0.3}\text{Gd}_{0.7})\text{SO}:\text{Ce}$  films in comparison with the LY of LSO:Ce films.

5. The main problem in the development of silicate film scintillators by LPE method using the traditional  $\text{PbO}-\text{B}_2\text{O}_3$  flux is connected with the significantly larger influence of  $\text{Pb}^{2+}$  flux dopant on the blue luminescence of  $\text{Ce}^{3+}$  ions in the silicate films than in the case of recently developed visible emitting YAG:Ce and LuAG:Ce garnet film scintillators.

*This is the main reason for the lower (by 2-3 times) LY of  $\text{Ce}^{3+}$  doped LSO:Ce and LGSO;Ce films in comparison with their best Y- or Gd-doped bulk crystal analogues.*

6. Therefore, the future development of blue-emitting scintillators based on  $\text{Ce}^{3+}$ -doped LSO and LGSO films ***strongly demands the use of alternative lead-free fluxes*** for their crystallization, for instant, BaO-based fluxes

## Characterization of BaO-based flux

### Advantages of lead-free BaO-based flux

- No energy transfer from  $\text{Ce}^{3+}$  centers or quenching of  $\text{Ce}^{3+}$  luminescence was observed in SCFs prepared from BaO-based flux;
- The strongly single-exponential decay of  $\text{Ce}^{3+}$  luminescence in these SCF is observed, with lifetime which are close to values of lifetimes for  $\text{Ce}^{3+}$  luminescence in bulk single crystal counterpart.

### Disadvantages of BaO-based flux

The fundamental problem of using of the BaO-based flux is significantly complicated SCF growth with respect to crystallization from the traditional PbO-based flux due to very **high viscosity and surface tension** of the BaO-based melt as well as **low SCFs growth rate**. As a consequence, worse surface morphology and uniformity of properties is noted at higher ( $> 5 \mu\text{m}$ ) thickness of SCF.

### Unclear moments of growth from the BaO-based fluxes

The hetero-epitaxial crystallization of LSO based SCFs onto cheaper YSO substrates not yet performed up to now.

**Thank you for attention !**

**Спасибо за внимание !**

**Дякую за увагу !**